Highly conductive p-type amorphous oxides from low-temperature solution processing

Jinwang Li, Eisuke Tokumitsu, Mikio Koyano, Tadaoki Mitani, and Tatsuya Shimoda

Citation: Appl. Phys. Lett. **101**, 132104 (2012); doi: 10.1063/1.4754608
View online: http://dx.doi.org/10.1063/1.4754608
View Table of Contents: http://apl.aip.org/resource/1/APPLAB/v101/i13
Published by the American Institute of Physics.

Highly conductive p-type amorphous oxides from low-temperature solution processing

Jinwang Li (李金望),[1,2,a)] Eisuke Tokumitsu (徳光永輔),[1,2,3,4] Mikio Koyano (小矢野幹夫),[2,3] Tadaoki Mitani (三谷忠興),[1] and Tatsuya Shimoda (下田達也)[1,2,3]
[1]*Japan Science and Technology Agency (JST), ERATO, Shimoda Nano-Liquid Process Project, 2-5-3 Asahidai, Nomi, Ishikawa 923-1211, Japan*
[2]*Green Devices Research Center, Japan Advanced Institute of Science and Technology, 1-1 Asahidai, Nomi, Ishikawa 923-1292, Japan*
[3]*School of Materials Science, Japan Advanced Institute of Science and Technology, 1-1 Asahidai, Nomi, Ishikawa 923-1292, Japan*
[4]*Precision and Intelligence Laboratory, Tokyo Institute of Technology, 4259-R2-19 Nagatsuta, Midori-ku, Yokohama 226-8503, Japan*

(Received 2 August 2012; accepted 6 September 2012; published online 26 September 2012)

We report solution-processed, highly conductive (resistivity 1.3–3.8 mΩ cm), p-type amorphous A-B-O (A = Bi, Pb; B = Ru, Ir), processable at temperatures (down to 240 °C) that are compatible with plastic substrates. The film surfaces are smooth on the atomic scale. Bi-Ru-O was analyzed in detail. A small optical bandgap (0.2 eV) with a valence band maximum (VBM) below but very close to the Fermi level (binding energy $E_{VBM} = 0.04$ eV) explains the high conductivity and suggests that they are degenerated semiconductors. The conductivity changes from three-dimensional to two-dimensional with decreasing temperature across 25 K. © *2012 American Institute of Physics*. [http://dx.doi.org/10.1063/1.4754608]

An ideal fabrication process for electronics is simple printing under atmospheric conditions and at low temperatures, which enables low cost, low energy input, and high throughput production of large-area devices on flexible substrates. Solution processing of functional materials is the precondition for this process, and nanosize scalability is a necessity to compete with conventional silicon techniques. Pattern sizes of polycrystalline materials are restricted because of their crystal dimensions (typically > 20 nm), and thus amorphous materials are required. Solution methods for semiconducting[1–5] and insulating[6,7] amorphous oxides with processing temperatures down to 230 °C and 300 °C, respectively, have been reported, but they have not yielded amorphous conductive electrode materials. On the other hand, p-type oxides have been intensively investigated,[8–12] but their solution processing remains a challenge. Here, we report p-type amorphous A-B-O (a-ABO, A = Bi, Pb; B = Ru, Ir) oxides with low resistivity (1.3–3.8 mΩ cm) by using solution processing at temperatures as low as 240 °C; these oxides are suitable for electrode and hole injection applications.

Solution-processed, printed silicon films and transistors have been demonstrated.[13] Today, advanced printing techniques, e.g., imprinting,[14] that have a high potential for simple and fast fabrication of devices in air, provided the appropriate materials are developed, are available. Metals, conductive oxides, carbon (graphene and carbon nanotubes), and conductive organics may be candidate materials for electrode conductors. However, with regards to the ability for solution processing in air and the stability to endure subsequent processing of other layers, only two noble metals (platinum[15] and silver[16]), aluminum,[17] and oxides such as tin-doped indium oxides (ITO)[18] and $LaNiO_3$ (Ref. 19) are available, all of which are polycrystalline. While organics can be solution-processed in air, they suffer from poor electrical and thermal stabilities. Nevertheless, polycrystalline materials cannot be scaled down to the required size, and furthermore, these oxides require high annealing temperatures (>400 °C). In contrast, amorphous materials have, in addition to unlimited scalability, various other advantages: (1) they have smooth surfaces and thus can achieve superior interface properties, (2) they can be uniformly deposited over large areas, and (3) they are free of problematic grain boundaries. All-amorphous-oxide thin film transistors (TFTs) deposited by sputtering have been demonstrated.[20] A conductive amorphous material from solution processing in air, however, is still urgently needed.

Regarding p-type oxides, in addition to their application as p-channel materials in oxide TFTs, they can be used as electrodes, given sufficient conductivity. In particular, in certain devices such as solar cells, p-type electrodes are required for hole injection. In n-channel TFTs, p-type gate electrodes, rather than n-type electrodes, are used in order to avoid depletion at the gate–insulator contact. So far, p-type oxides have been synthesized only by vacuum deposition techniques. A major reason for the failure of their solution processing is that they are mostly based on metal ions in valence states (Cu 1+, Sn 2+) that are unstable under ambient conditions.[8–10] Among the existing p-type oxides, only Zn-Rh-O (resistivity ~500 mΩ cm)[11,12] and Zn-Co-O (~50 mΩ cm)[21] are amorphous.

In the context of research toward printed electronics, we have studied low-temperature solution-deposition techniques for films and patterns (e.g., platinum,[15] aluminium,[17] and lead zirconate titanate).[22,23] In order to produce a conductive amorphous oxide from solution, we focused on Ru oxides. Crystalline RuO_2 is a well-known electrode material that

a)Author to whom correspondence should be addressed. Electronic mail: lijw@jaist.ac.jp.

exhibits metallic conduction. Initially, we found that the amorphous phase of RuO_2 is unstable and only crystalline films can be obtained via solution processing even at low processing temperatures below 300 °C. We then used lanthanide elements (Ln, except Ce) to stabilize the amorphous phase, and as a result, amorphous Ln-Ru-O (a-LnRuO), which are stable up to 800 °C processable around 400 °C and are p-type semiconductors with the lowest room temperature (RT) DC resistivity of 16 mΩ cm (Ref. 24) were prepared. Amorphous Ln-Ir-O showed similar conduction. These oxides are highly interesting with regards to many of their features, including their electron structures, which distinguish them from previous p-type oxides;[24] however, their resistivity is not low enough for use in practical applications, and their processing temperature is too high for deposition on flexible substrates.

It is known that the conduction of ruthenium pyrochlore, $A_2Ru_2O_7$, is sensitive to the type of A element. These compounds are semiconducting for A = Y and the lanthanides Pr–Lu (La-Ru-O does not crystallize into pyrochlore), and weakly metallic for A = Bi and Pb. The origin of the difference has been under debate[25] and is likely related to the hybridization of the Bi/Pb 6p band with the Ru 4d band.[26,27] The Ln of the above-mentioned oxides was thus replaced with Bi and Pb, leading to low-resistivity amorphous oxides produced at low temperatures.

To deposit the films, solutions were prepared under an ambient atmosphere by simply dissolving the corresponding metal acetates in propionic acid with monoethanolamine as a chelating agent. Next, the solutions were spin coated onto SiO_2/Si or SiO_2 glass substrates and then dried and annealed in air or oxygen. (See supplementary material[28] for the details of experimental methods.) The x-ray diffraction (XRD) patterns (Fig. 1(a)) show no peaks for the BiRuO and PbRuO films annealed up to 400 °C or for the BiIrO film annealed up to 500 °C. Because nanocrystals may not be detected by XRD, transmission electron microscopy (TEM) with electron diffraction (ED) analysis was also performed, which confirmed that the films annealed below these temperatures were amorphous in the absence of nanocrystals (Figs. 1(b)–1(d)). The films annealed at 500 °C (BiRuO and PbRuO) or 550 °C (BiIrO) crystallized into $Bi_3Ru_3O_{11}$, $Pb_2Ru_2O_{6.5}$, and $Bi_2Ir_2O_7$, respectively (Fig. 1(a)). Atomic force microscopy (AFM) revealed that the amorphous films are highly smooth, with a typical root mean square (RMS) roughness of approximately 0.5 nm and a peak-valley (P-V) roughness of a few nanometers over a scanning area of $1 \times 1\ \mu m^2$ (Fig. 1(e)).

The resistivity values of 20-nm-thick films annealed stepwise from 230 °C to 500 °C in air, with a holding time of 5 min at each step, are displayed in Fig. 2(a). The lowest necessary annealing temperature for a-BiRuO, a-PbRuO, and a-BiIrO are 240 °C, 290 °C, and 350 °C, respectively, resulting in RT DC resistivities of 3.8, 1.7, and 3.8 mΩ cm, respectively. Further annealing at higher temperatures reduced the resistivities to 1.8, 1.4, and 1.8 mΩ cm, respectively. Thicker films (200 nm) of a-BiRuO (annealed at 400 °C for 30 min) and a-PbRuO (annealed at 350 °C for 30 min) showed resistivities of 1.7 and 1.3 mΩ cm, respectively, which are similar to the values of the 20-nm-thick films, indicating that highly uniform and ultrathin (≤20 nm) films can be prepared. The resistivity of a-BiRuO has nearly reached the value of crystalline bulk $Bi_3Ru_3O_{11}$ (~1.4 mΩ cm),[29] which suggests that the films are of high quality. In addition, the Seebeck coefficient values are positive (Fig. 2(b)), revealing that these films are p-type. (Confirmation of reliability of the Seebeck measurement is shown in Fig. S1 in the supplementary material.)[25] In p-type oxides, the low resistivity values of these amorphous oxides are matched only by epitaxial LaCuOSe:Mg annealed at a high temperature of 1000 °C (1.1 mΩ cm).[30]

For comparison, a-BiRuO films were also prepared by radio-frequency (RF) sputtering. The sample sputtered under optimum conditions exhibits a resistivity (1.5 mΩ cm after annealing at 400 °C) similar to that of the solution-processed samples (Fig. 2(a) inset), and is also p-type (Fig. 2(b)). It is very advantageous that highly conductive films of this oxide can be produced using a simple solution processing method, which is in contrast to other oxides such as ITO, for which sputtered samples show superior properties over solution-processed films.[17]

The elemental compositions of the films are listed in Table I. For a-BiRuO annealed at 260 °C, residual carbon

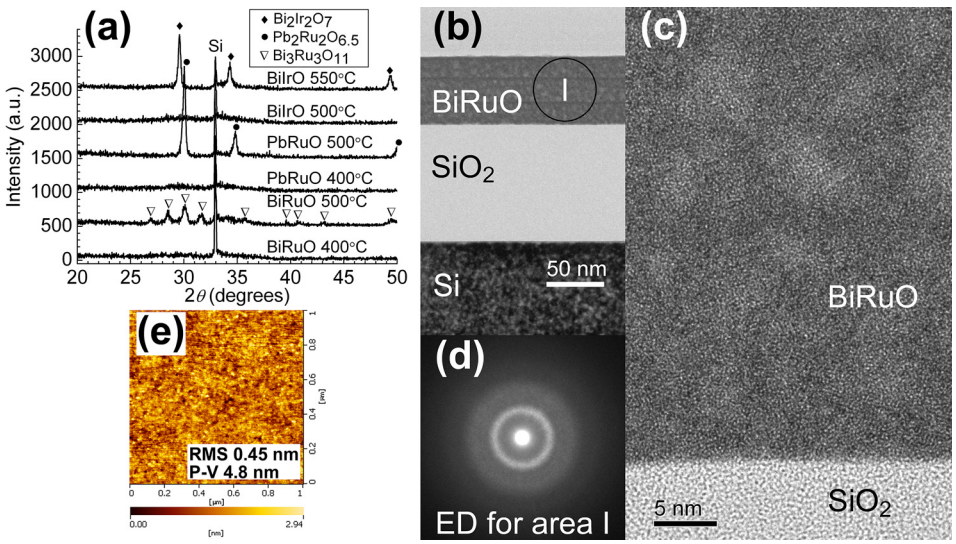

FIG. 1. Phase and morphology analyses of the oxides. (a) XRD patterns. (b)–(e) TEM images at low (b) and high (c) magnifications, and electron diffraction pattern (d) and AFM image (e) for 400 °C-annealed BiRuO.

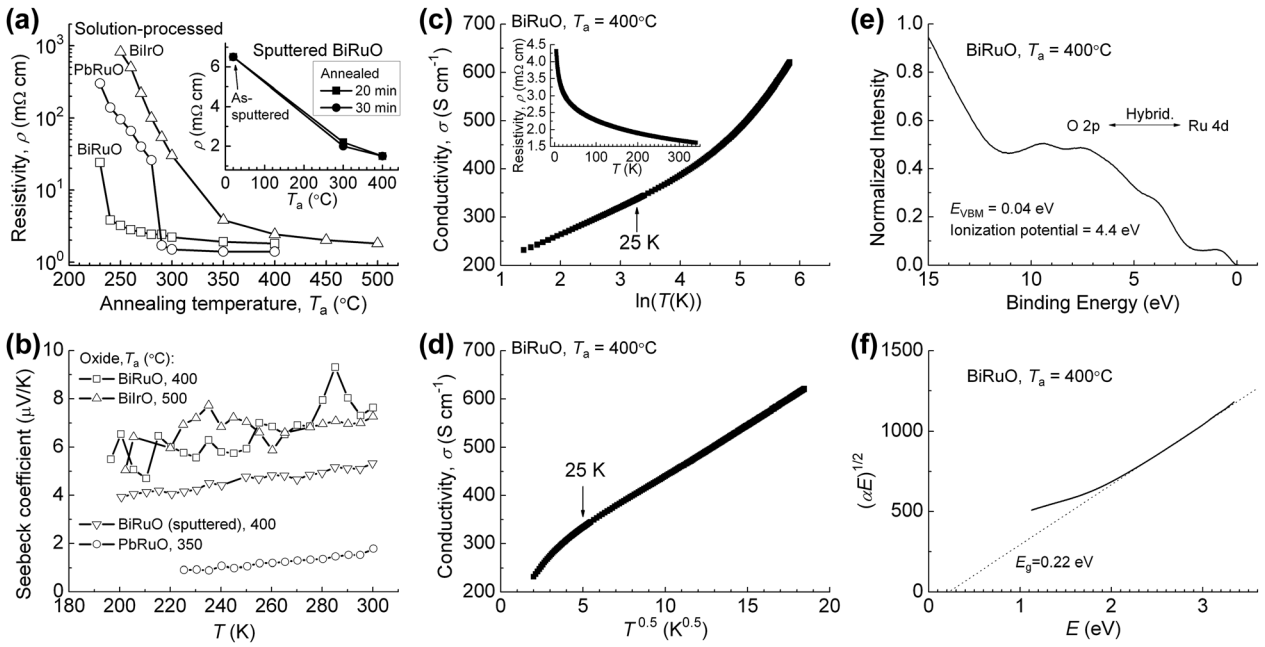

FIG. 2. Electrical properties and band structure analysis of the oxides. (a) RT DC resistivity as a function of annealing temperature. The inset is for sputtered BiRuO films prepared for comparison. (b) Seebeck coefficient as a function of measurement temperature. (c)–(f) Temperature dependence of conductivity (c)–(d), UPS analysis (e), and Tauc plot for the optical band gap analysis (f) of a 400 °C-annealed a-BiRuO film. The conductivity shows two-dimensional behavior (ln T dependence of σ) below 25 K (c) and three-dimensional behavior ($T^{1/2}$ dependence of σ) above 25 K (d), respectively. The inset in panel (c) shows the resistivity against temperature.

was not detected and only a small amount of residual hydrogen remained, indicating nearly complete conversion of the sample to the oxide. The 400 °C-annealed a-BiRuO, showing no detectable carbon and hydrogen, was completely decomposed into the oxide (C and H detection limit: 1.5 at. %). In contrast, for a-PbRuO and a-BiIrO, a significant amount of C was found even after annealing at 350 °C and 500 °C, respectively. This result is in consistent with the above observation that BiRuO can be annealed at temperatures lower than those of PbRuO and BiIrO. In all of the solution-processed samples, the oxygen content is much higher than that of the sputtered counterparts and the calculated compositions, which may imply an unusual electronic structure of the solution-derived materials. The chlorine impurity originated from contaminants in the raw materials (metal acetates). The deviation in the Ru/Bi ratio (1.1) from the designed value (1.0) is attributed to experimental error.

The a-BiRuO film, whose annealing temperature is the lowest of those of the oxides prepared in this study, was further analyzed. The temperature dependence of resistivity (Fig. 2(c) inset) reveals that it is a semiconductor. The data do not follow the thermal activation model or the variable range hopping model. Instead, the conductivity, σ, can be described by the Anderson localization or the Coulomb interaction theory for disordered systems.[31] According to the theory, in a disordered system, the carrier wave function can be localized due to the loss of phase coherence caused by scattering by the random potential. In addition, interactions between carriers, which are characterized by the thermal diffusion length, are increased in a disordered system. Both the phase coherence length and the thermal diffusion length increase with decreasing temperature. In a disordered thin film where such a feature length is smaller than the film thickness, the conduction is three-dimensional with $T^{1/2}$ dependence of σ. In contrast, if the feature length is larger than the film thickness, the wave localization or the carrier interactions take place only in-plane (i.e., two dimensional, with ln$T$ dependence of σ). The a-BiRuO film shows a crossover from three-dimensional behavior above 25 K (Fig. 2(d)) to two-dimensional behavior at lower temperatures (Fig. 2(c)). This indicates that the phase coherence length or thermal diffusion length of the carrier exceeded the thickness

TABLE I. Composition of solution-processed oxide films. A sputtered a-BiRuO film is also listed for comparison.

Oxide	T_a (°C)[a]	Measured composition	Calculated O[b]
BiRuO	260	$BiRu_{1.13(5)}O_{4.6(3)}H_{0.20\ (5)}Cl_{0.10(2)}$	$BiRu_{1.1}O_{3.70}$ or $BiRu_{1.1}O_{3.88}$
	400	$BiRu_{1.11(5)}O_{4.7(3)}Cl_{0.10(2)}$	$BiRu_{1.1}O_{3.70}$ or $BiRu_{1.1}O_{3.88}$
BiRuO (sputtered)	400	$BiRu_{0.97(2)}O_{3.6(1)}Ar_{0.028(6)}$	$BiRuO_{3.50}$ or $BiRuO_{3.67}$
PbRuO	350	$PbRu_{1.10(5)}O_{4.0(3)}H_{0.11(2)}C_{0.15(5)}Cl_{0.08(1)}$	$PbRu_{1.1}O_{3.20}$ or $PbRu_{1.1}O_{3.88}$
BiIrO	500	$BiIrO_{4.0(3)}C_{0.26(5)}$[c]	$BiIrO_{3.50}$

[a]T_a represents the annealing temperature. All samples were annealed in air ($T_a \leq 400$ °C) or O_2 ($T_a = 500$ °C) for 30 min.
[b]The calculated O is the content of O required for the charge balance assuming the valence states of Bi 3+, Pb 2+, Ru 4+ and Ir 4+, or possibly higher valence states of Pb 3+ and Ru 4.33+.
[c]Bi and Ir could not be separated in the analysis; thus, the designed atomic ratio (Bi/Ir = 1) was used.

(60 nm) of this film sample below 25 K. More detailed study is certainly interesting.

Ultraviolet photoelectron spectroscopy (UPS) was used to analyze the valence band structure of a-BiRuO. The spectrum (Fig. 2(e)) shows that the Ru 4d state is centered at 0.9 eV and is hybridized with the O 2p (2.5–8 eV). Unlike the weakly metallic pyrochlore $Bi_2Ru_2O_7$, whose maximum of the Ru 4d band exceeds the Fermi level,[32] in amorphous a-BiRuO, the edge of Ru 4d is 0.04 eV below the Fermi level. In other words, in a-BiRuO, the hybridized O 2p and Ru 4d form the valence band, with a valence band maximum (VBM) very close to the Fermi level (binding energy $E_{VBM} = 0.04$ eV). This result is consistent with p-type conduction. Compared to a-LaRuO (Ru 4d centered at 1.6 eV, O 2p at 3–8 eV, and $E_{VBM} = 0.1$–0.2 eV),[21] the binding energy in a-BiRuO, noticeably Ru 4d (0.9 eV), shifts to lower values, resulting in a VBM that is much closer to the Fermi level. This difference may be attributed to the hybridization of Ru 4d with Bi 6p, as in the pyrochlore phases.[23,24] This difference would explain why the resistivity of a-BiRuO is one order lower than that of a-LaRuO. A feature centered at 9.5 eV may be assigned to O 2p associated with non-network O (O not in the RuO_6 network).

The UPS analysis gave an ionization potential of 4.4 eV for a-BiRuO, which is well in the range of existing p-type oxides ($< \sim 5.5$ eV).[33] The a-BiRuO film is not transparent and has a narrow optical bandgap of 0.2 eV, as determined by the Tauc plot of the UV-visible spectrum (Fig. 2(f)). Note that for most printed electronics, transparency is unnecessary.

Accordingly, the conduction of a-BiRuO is different from that of its crystalline counterpart phases, $Bi_3Ru_3O_{11}$ (Ref. 25) and $Bi_2Ru_2O_7$ (Ref. 24), which are both metallic. The existence of a small optical bandgap with very small E_{VBM} in a-BiRuO suggests that it is a degenerated semiconductor with localized states around the Fermi level.

In summary, using simple solution processing, we have produced highly conductive (resistivity 1.3–3.8 mΩ cm), p-type amorphous A-B-O (a-ABO, A = Bi, Pb; B = Ru, Ir), processable at low temperatures (down to 240 °C) that are compatible with plastic substrates. The surfaces are smooth on the atomic scale. Detailed analysis of a-BiRuO revealed that the valence band maximum is composed of Ru 4 d electrons, which is only 0.04 eV below the Fermi level. The bandgap is rather narrow (0.2 eV). The conductivity shows interesting crossover from three-dimensional above 25 K to two-dimensional below 25 K. We expect that these amorphous oxides will find applications in printed electronics, e.g., as electrodes in nanodevices and solar cells. As an example, using a-BiRuO as the electrode, together with other solution-processed insulating and semiconducting amorphous oxides, we have been able to fabricate high-performance TFTs. The detailed results of the TFTs will be reported elsewhere.

The authors thank Professor S. Katayama for helpful comments. The assistance of co-workers in measurements is acknowledged.

[1]S. Jeong, Y.-G. Ha, J. Moon, A. Facchetti, and T. J. Marks, Adv. Mater. **22**, 1346 (2010).
[2]K. K. Banger, Y. Yamashita, K. Mori, R. L. Peterson, T. Leedham, J. Rickard, and H. Sirringhaus, Nature Mater. **10**, 45 (2011).
[3]M.-G. Kim, M. G. Kanatzidis, A. Facchetti, and T. J. Marks, Nature Mater. **10**, 382 (2011).
[4]M.-G. Kim, H. S. Kim, Y.-G. Ha, J. He, M. G. Kanatzidis, A. Facchetti, and T. J. Marks, J. Am. Chem. Soc. **132**, 10352 (2010).
[5]Z. L. Mensinger, J. T. Gatlin, S. T. Meyers, L. N. Zakharov, D. A. Keszler, and D. W. Johnson, Angew. Chem. Int. Ed. **47**, 9484 (2008).
[6]C. Avis and J. Jang, J. Mater. Chem. **21**, 10649 (2011).
[7]K. Jiang, J. T. Anderson, K. Hoshino, D. Li, J. F. Wager, and D. A. Keszler, Chem. Mater. **23**, 945 (2011).
[8]H. Kawazoe, M. Yasukawa, H. Hyodo, M. Kurita, H. Yanagi, and H. Hosono, Nature **389**, 939 (1997).
[9]H. Kawazoe, H. Yanagi, K. Ueda, and H. Hosono, MRS Bull. **25**, 28 (2000).
[10]Y. Ogo, H. Hiramatsu, K. Nomura, H. Yanagi, T. Kamiya, M. Kimura, M. Hirano, and H. Hosono, Phys. Status Solidi A **206**, 2187 (2009).
[11]S. Narushima, H. Mizoguchi, K. Shimizu, K. Ueda, H. Ohta, M. Hirano, T. Kamiya, and H. Hosono, Adv. Mater. **15**, 1409 (2003).
[12]T. Kamiya, S. Narushima, H. Mizoguchi, K. Shimizu, K. Ueda, H. Ohta, M. Hirano, and H. Hosono, Adv. Funct. Mater. **15**, 968 (2005).
[13]T. Shimoda, Y. Matsuki, M. Furusawa, T. Aoki, I. Yudasaka, H. Tanaka, H. Iwasawa, D. Wang, M. Miyasaka, and Y. Takeuchi, Nature **440**, 783 (2006).
[14]Z. Hu, M. Tian, B. Nysten, and A. M. Jonas, Nature Mater. **8**, 62 (2009).
[15]Z. Shen, J. Li, Y. Matsuki, and T. Shimoda, Chem. Commun. **47**, 9992 (2011).
[16]Y. Wu, Y. Li, and B. S. Ong, J. Am. Chem. Soc. **129**, 1862 (2007).
[17]Z. Shen, Y. Matsuki, and T. Shimoda, J. Am. Chem. Soc. **134**, 8034 (2012).
[18]M. J. Alam and D. C. Cameron, Thin Solid Films **420**, 76 (2002).
[19]T. Miyasako, B. N. Q. Trinh, M. Onoue, T. Kaneda, P. T. Tue, E. Tokumitsu, and T. Shimoda, Appl. Phys. Lett. **97**, 173509 (2010).
[20]J. Liu, D. B. Buchholz, J. W. Hennek, R. P. H. Chang, A. Facchetti, and T. J. Marks, J. Am. Chem. Soc. **132**, 11934 (2010).
[21]S. H. Kim, J. A. Cianfrone, P. Sadik, K.-W. Kim, M. Ivill, and D. P. Norton, J. Appl. Phys. **107**, 103538 (2010).
[22]J. Li, H. Kameda, B. N. Q. Trinh, T. Miyasako, P. T. Tue, E. Tokumitsu, T. Mitani, and T. Shimoda, Appl. Phys. Lett. **97**, 102905 (2010).
[23]H. Kameda, J. Li, D. H. Chi, A. Sugiyama, K. Higashimine, T. Uraga, H. Tanida, K. Kato, T. Kaneda, T. Miyasako, E. Tokumitsu, T. Mitani, and T. Shimoda, J. Eur. Ceram. Soc. **32**, 1667 (2012).
[24]J. Li, T. Kaneda, E. Tokumitsu, M. Koyano, T. Mitani, and T. Shimoda, Appl. Phys. Lett. **101**, 052102 (2012).
[25]R. J. Cava, Dalton Trans. **2004**, 2979.
[26]J. S. Lee, S. J. Moon, T. W. Noh, T. Takeda, R. Kanno, S. Yoshii, and M. Sato, Phys. Rev. B **72**, 035124 (2005).
[27]M. Tachibana, Y. Kohama, T. Shimoyama, A. Harada, T. Taniyama, M. Itoh, H. Kawaji, and T. Atake, Phys. Rev. B **73**, 193107 (2006).
[28]See supplementary material at http://dx.doi.org/10.1063/1.4754608 for the details of experimental methods, including confirmation of reliability of the Seebeck measurement.
[29]T. Fujita, K. Tsuchida, Y. Yasui, Y., Kobayashi, and M. Sato, Physica B **329–333**, 743 (2003).
[30]H. Hiramatsu, K. Ueda, H. Ohta, M. Hirano, M. Kikuchi, H. Yanagi, T. Kamiya, and H. Hosono, Appl. Phys. Lett. **91**, 012104 (2007).
[31]P. A. Lee and T. V. Ramakrishnan, Rev. Mod. Phys. **57**, 287–337 (1985).
[32]J. Park, K. H. Kim, H.-J. Noh, S.-J. Oh, J.-H. Park, H.-J. Lin, and C.-T. Chen, Phys. Rev. B **69**, 165120 (2004).
[33]H. Hosono and T. Kamiya, Ceramics **38**, 825 (2003).